Abiotic and biotic sources influencing spring new particle formation in North East Greenland

Dall´Osto, M.; Simo, R.; Harrison, Roy M.; Beddows, D. C.S.; Saiz-Lopez, A.; Lange, R.; Skov, H.; Nøjgaard, J. K.; Nielsen, I. E.; Massling, A.

DOI:
10.1016/j.atmosenv.2018.07.019

Atmospheric Environment 190 (2018) 126–134

Contents lists available at ScienceDirect

Atmospheric Environment

journal homepage: www.elsevier.com/locate/atmosenv

Abiotic and biotic sources influencing spring new particle formation in North East Greenland

M. Dall´Osto[a,*], R. Simo[a], Roy M. Harrison[b,1], D.C.S. Beddows[b], A. Saiz-Lopez[c], R. Lange[d], H. Skov[d], J.K. Nøjgaard[d], I.E. Nielsen[d], A. Massling[d]

[a] Institute of Marine Sciences, CSIC, Passeig Marítim de la Barceloneta, 37-49. E-08003, Barcelona, Spain
[b] National Center for Atmospheric Sciences, University of Birmingham, Edgbaston, Birmingham, B15 2TT, United Kingdom
[c] Department of Atmospheric Chemistry and Climate, Institute of Physical Chemistry Rocasolano, CSIC, Serrano 119, 28006, Madrid, Spain
[d] Department of Environmental Science, Aarhus University, Frederiksborgvej 399, 4000, Roskilde, Denmark

ARTICLE INFO

Keywords:
Arctic
New particle formation
Sea ice
Snow
Iodine
MSA

ABSTRACT

In order to improve our ability to predict cloud properties, radiative balance and climate, it is crucial to understand the mechanisms that trigger the formation of new particles and their growth to activation sizes. Using an array of real time aerosol measurements, we report a categorization of the aerosol population taken at Villum Research Station, Station Nord (VRS) in North Greenland during a period of 88 days (February–May 2015). A number of New Particle Formation (NPF) events were detected and are herein discussed. Air mass back trajectories analysis plotted over snow-sea ice satellite maps allowed us to correlate early spring (April) NPF events with air masses travelling mainly over snow on land and sea ice, whereas late spring (May) NPF events were associated with air masses that have passed mainly over sea ice regions. Concomitant aerosol mass spectrometry analysis suggests methanesulfonic acid (MSA) and molecular iodine (I_2) may be involved in the NPF mechanisms. The source of MSA was attributed to open leads within the sea ice. By contrast, iodine was associated with air masses over snow on land and over sea ice, suggesting both abiotic and biotic sources. Measurements of nucleating particle composition as well as gas-phase species are needed to improve our understanding of the links between emissions, aerosols, cloud and climate in the Arctic; therefore our ability to model such processes.

1. Introduction

In the Arctic, clouds are the dominant factor in the control of the incoming and outgoing energy balance at the Earth's surface (Intrieri et al., 2002). Aerosols act as cloud condensation nuclei (CCN), upon which cloud droplets are formed (Ramanathan et al., 2001). It is long established that aerosols and their cloud seeding role, the so-called indirect aerosol effect, have a substantial impact on the Earth's albedo and climate (Charlson et al., 1987). However, what regulates the number of aerosol particles and their capability to act as CCN still is poorly known and constitutes one of the largest sources of uncertainty in climate understanding and modelling (Carslaw et al., 2013). In the Arctic climate system the picture is even more complicated because there are many dynamic inter-connections between processes occurring on partly snow-covered land and in sea ice and the ocean. All of these environmental components, and their changes over time (Serreze and Stroeve, 2015) influence not only the surface albedo but also the composition and radiative properties of the atmosphere.

New particle formation (NPF), if accompanied by stabilization and growth, increases aerosol number concentrations in the atmosphere (Kulmala et al., 2004; Spracklen et al., 2006), providing a pool of secondary aerosols with potential to increase CCN population. Background particle concentrations in the summertime Arctic are typically very low ($\sim 100\,cm^{-3}$). Cloud properties in this region are therefore highly sensitive to the mechanisms by which new particles form and grow (Merikanto et al., 2009). A better understanding of the physical and chemical processes leading to a higher nucleation potential requires detailed knowledge about aerosol precursor emissions from the different types of surfaces in the Arctic environment. In the Arctic lower troposphere, nucleation and Aitken mode particles dominate the size distribution during summer, in contrast to the accumulation mode-dominated winter and spring (Ström et al., 2011; Heintzenberg and

* Corresponding author.
E-mail address: dallosto@icm.csic.es (M. Dall´Osto).
[1] Also at: Department of Environmental Sciences/Centre of Excellence in Environmental Studies, King Abdulaziz University, PO Box 80203, Jeddah, 21589, Saudi Arabia.

https://doi.org/10.1016/j.atmosenv.2018.07.019
Received 9 January 2018; Received in revised form 2 July 2018; Accepted 9 July 2018
Available online 20 July 2018

Leck, 2012; Tunved et al., 2013; Leaitch et al., 2013). At very high latitudes in sea ice-covered regions or near the marginal ice zone, it has also been suggested that small primary particles may arise from bubble bursting (Leck and Bigg, 1999). Particle nucleation has been observed in this region as well (Heintzenberg et al., 2015; Wiedensohler et al., 1996). Recently, Dall'Osto et al. (2018) categorized the aerosol population via cluster analysis of aerosol number size distributions taken at Villum Research Station, Station Nord (VRS) in North Greenland during a 7 year record (2010–2016). Most NPF events (annually 9% of the time, up to 39% during summer months) were associated with air mass back trajectories passing over open water and melting sea ice regions, suggesting these regions as the main source. The origin of these ultrafine particles seems to be marine biological activities within the open leads in the pack ice and/or along the melting marginal sea ice zone (MIZ). The results from the period 2010–2016 at VRS are in line with recent results from the period 2000–2010 at the Zeppelin Mountain Station (Dall'Osto et al., 2017a). However, it is important to stress that the NPF source regions and corresponding precursor components are still a topic of intense research, and not only include emissions of precursor gases associated with biological communities on or near sea ice margins (Dall'Osto et al., 2017a; b; Levasseur, 2013), but also seabird colonies (Croft et al., 2016; Weber et al., 1998) and intertidal zones (O'Dowd et al., 2002; Allan et al., 2015; Sipilä et al., 2016). Overall, there is an increasing number of studies reporting observations of secondary organic components of the Arctic aerosol (Leaitch et al., 2018) from emissions of biogenic volatile organic compounds (BVOCs; e.g., isoprene and terpenes), including oxygenated VOCs (OVOCs; Mungall et al., 2017) and trimethylamines (Köllner et al., 2017). Additionally, it is important to stress that nucleation events in Greenland have been also associated with air masses that travelled over snow regions, and mechanisms based on gas precursors released from the snowpack were suggested (Ziemba et al., 2010).

Traditionally, experiments conducted in the Arctic have mainly focused on the Arctic Haze phenomenon during late winter and spring and on NPF events occurring mainly only during summer (Tunved et al., 2013; Freud et al., 2017). Here, for the first time we focus our attention on springtime NPF events in coastal North Greenland: we identify these events by aerosol size distributions, characterize key chemical components, and relate them to air mass trajectories over categorized surfaces.

2. Experimental measurements

Aerosol measurements were undertaken at VRS, Greenland. Located at 81° 36′ N, 16° 40' W the station is situated in the most north-eastern part of Greenland, on the coast of the Fram Strait. The sampling took place about 2 km south-west of the main facilities of the Station Nord military camp in two different sampling stations. Measurements were shifted in summer 2015 from the original hut called "Flygers hut" to the new air observatory, 300 m west of "Flygers hut". The sampling locations are upwind from the station the vast majority of the time (97.3%). Detailed descriptions of the site and analysis of predominant wind directions are available in Nguyen et al. (2016) and Nguyen et al. (2013). VRS at Station Nord is a unique Arctic station located close to sea level at the ice stream from the Arctic Ocean. VRS is furthermore always located north of the polar Vortex representing the conditions of the high Arctic throughout the whole year.

Detailed information about scanning mobility particle sizer (SMPS) measurements can be found elsewhere (Nguyen et al., 2016). Measurement of particle number size distributions at Station Nord was initiated in July 2010 using a TROPOS-type Mobility Particle Size Spectrometer as described in Wiedensohler et al. (1996). Soot particle aerosol mass spectrometer (Aerodyne, SP-AMS) was deployed for four months over the period February–June 2015. The instrument is described in details elsewhere. The SP2 provides rBC mass loadings, particle number concentrations, and size distribution measurements, though these measurements are constrained by single particle detection limits of ~0.7 fg/particle (Schwarz et al., 2010). The SP-AMS is described in detail elsewhere (Onasch et al., 2012). In this study, high-resolution (HR) mass concentrations of SO_4^{2-}, NO_3^-, NH_4^+, organics, Cl, rBC (reflactive black carbon), and signals for I_2 and MSA are obtained from the SP-AMS. The SP-AMS was operated in 2 min laser off and 2 min laser on in V-mode and alternated between the mass spectrum mode and the particle time-of-flight (pToF) to obtain PM_1 (particulate matter with diameter below 1 μm) concentration and particle size distribution, respectively. The data was analyzed with the standard AMS Igor Pro-based (version 6.35 Wavemetrics, Inc) software SQUIRREL (version 1.57G) and PIKA (version 1.16H). The analysis was treated with general accepted principles described in DeCarlo et al. (2006), Jimenez et al. (2003) and Onasch et al. (2012).

Using the BADC Trajectory Service (British Atmospheric Data Centre Trajectory Service), 5 day back trajectories arriving at VRS station were calculated arriving at 100m altitude (hourly resolution). The length of the back-trajectory calculation is chosen as a balance between the typical lifetime of the aerosols in the Arctic troposphere, which is up to two weeks (shorter in summer and longer in winter/spring) for the accumulation-mode particles, and the increasing uncertainty in the calculation the further back in time it goes. Simple calculations were also made for each of the 5-day back trajectories using daily Arctic maps of gridded sea ice information. For each of the positions alone each of the trajectories the sea ice information was logged into a file from which the exposure to sea ice of all the air masses arriving at SN could be calculated. The Polar Stereographic map of the Northern Hemisphere classified each of 1024x1024 24 km grid cells as land, sea, ice or snow ice, and from this, the percentage of time each clustered back trajectory spent over each type could be calculated. The snow and ice coverage values were produced by the NOAA/NESDIS Interactive Multisensor Snow and Ice Mapping System (IMS) developed under the direction of the Interactive Processing Branch (IPB) of the Satellite Services Division (SSD). A similar calculation was repeated but using daily maps of sea ice percentage concentration measured on a 12.5 km grid. These Arctic polar sterographic maps of 12.5 km resolution contained sea ice concentration, available since 1992. The percentages assigned from these maps to each trajectory step allow a 'spectrum' of sea ice concentration of 5% width from 0 to 100% to be calculated for each of the trajectory clusters.

3. Results and discussion

3.1. NPF overview

K-means cluster analysis (Dall'Osto et al., 2018a; Lange et al., 2018) of particle number size distributions using 33,678 hourly distributions collected over 7 years (2010–2016, 55% data coverage during the period, see Nguyen et al., 2016) was carried out. Briefly, the K-means method aims to minimize the sum of squared distances between all points and the cluster centre. In order to choose the optimum number of clusters the Dunn-Index (DI) was used. The DI aims to identify dense and well-separated clusters. DI is defined as the ratio between the minimal intercluster distance to maximal intracluster distance. Consequently, we wanted to find the clustering which maximizes this index. The use of cluster analysis was justified in this work using a Cluster Tendency test (Beddows et al., 2009; Dall'Osto et al., 2011). Based on such cluster analysis, we identified eight categories of aerosol number size distributions (Dall'Osto et al., 2018a), and subsequently overlapped them with the time period where the SP-AMS was operating between 21st February 2015 and 23rd May 2015 (88 days in total). During this winter-spring period, 69 days (79%) were classified as Arctic Haze, carrying the highest total number concentration in the accumulation mode (> 100 nm, Fig. 1), peaking at about 170 nm and unimodal in appearance (Lange et al., 2018). Only 12 days (14%) were classified as "pristine" Arctic conditions (Fig. 1), characterized by very low particle

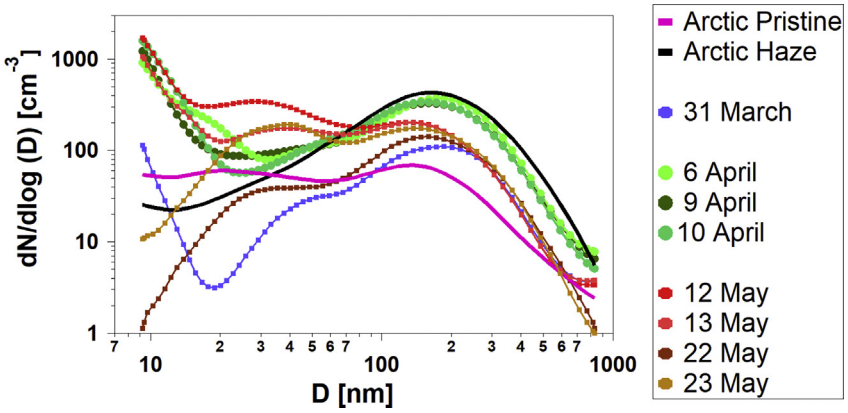

Fig. 1. Daily average size distributions (9–915 nm) obtained at Station Nord with an SMPS for days of new particle formation events, and average size distributions for the aerosol categories "Arctic Accumulation Haze" and "Arctic pristine" conditions described in Dall'Osto et al. (2018b) and Lange et al. (2018).

number concentrations $N_{9–915nm}$ ($< 100\,cm^{-3}$) and aerosol number distributions across different sizes, with minor modes at 35 nm and 135 nm. The K-means clustering analysis detected only NPF events occurring during few days, two in April (9th, 10th) and two in May (12th, 13th), apportioning only about 5% of total sampling time. NPF events were not detected in the months of February and March. However, by visual inspection of SMPS data, we were able to detect a number of additional events not successfully classified by the clustering method. The average daily size distributions of the NPF events are shown in Fig. 1. One event (31 March 2015) was characterized by small particles in very low particle number concentrations, whereas one event was characterized by already grown particles (about 20–25 nm growing over 30 h at about $0.75\,nm\,h^{-1}$ till about 45 nm, discussed in next sections). Overall, average particle number concentrations in the smallest SMPS bins ($N_{9–15nm}$) were about 60% lower than in similar NPF events detected in summer and described elsewhere (Dall'Osto et al., 2018a).

It is worth noting that some NPF events (especially the one detected in early spring - March, April) did not grow to particles larger than about 10–30 nm. A previous study made at Summit (Greenland, 3200 m above sea level) also reported four growth events with average aerosol growth rate between 0.09 and $0.3\,nm\,h^{-1}$ (Ziemba et al., 2010), possibly a result of the distance from sources of condensable vapour. It is also worth to point out that ozone concentrations measured by Ziemba et al. (2010) suggested that the detected particle growth events were not due to direct transport from the upper atmosphere. The hourly evolution of the events occurred mainly in the early morning and evening. Almost 24h light conditions occur at the location (81ºN) during at the season of the events (April–May), suggesting that insolation may not be a factor limiting NPF. The reasons for limited growth (not beyond 20–40 nm) are not known at this stage. The condensation sink (CS, the rate at which vapours condense on the available particle surface) is a very important factor influencing the nucleation process. Homogeneous nucleation is unlikely to occur in environments with a high condensation sink because under such circumstances, condensable molecules and clusters are likely to attach to existing surfaces rather than self-nucleate to form new particles (Dall'Osto et al., 2018a). It is interesting to note that the April NPF events occur with higher Condensation Sink (CS) relative to the May ones ($1.3\ 10^{-3}\ s^{-1}$ and $9.5\ 10^{-4}\ s^{-1}$, respectively; CS calculation formula is reported in Dall'Osto et al., 2013), as reflected in the co-existing large aerosol accumulation mode shown in Fig. 1 for the April NPF events. Summer CS for NPF events at VRS station are in the order of $8.9\ 10^{-4}\ s^{-1}$ (Dall'Osto et al., 2018b), and of about $4\ 10^{-4}\ s^{-1}$ for station Zeppelin (ZEP, Dall'Osto et al., 2017a). Previous studies argued that the CS may not be a factor that directly limits the NPF in this region (Collins et al., 2017). Another possibility for limited growth is the lack of chemical substances involved in the growth ($\sim > 10$ nm) of newly nucleated particles to tens of nanometres in diameter. Although in a more terrestrially-influenced environment (Tiksi, Russian Arctic), particle formation rates were the highest in spring, while the particle growth rates peaked in summer (Asmi et al., 2016). It is also important to remember that NPF generally occurs through the rapid photochemical production of low vapour pressure secondary material such that stable molecular clusters are able to grow to viable sizes (nm) (Kulmala et al., 2004; Allan et al., 2015). As they grow, the freshly nucleated particles act as sinks for the secondary condensable material, potentially shutting off any further nucleation. Information on the nature of condensable vapours and the evidence of their sources in the Arctic environment is currently lacking (Burkart et al., 2017a; b; Willis et al., 2017).

3.2. Air mass back trajectory analysis

Motivated by identifying possible sources of the NPF events detected in April and May, we computed the corresponding air mass back trajectories. Hourly air masses travelling 96 h before arriving at Station North were plotted for each daily average SMPS size distributions shown in Fig. 1 (total 24 air mass back trajectories per day). Two different analyses for each day of the NPF events are presented. First, we calculated how long each air mass travelled over zones categorized by their surface characteristics, namely land only, land covered by snow, sea ice and open water. Second, we calculated the amount of time spent by the associated air mass trajectory over the sea ice regions (see experimental method, section 2).

Results are shown in Fig. 2 for three selected events detected on 31 March (a, b), 9–10 April 2015 (c, d) and 22–23 May 2015 (e, f). The first NPF event is characterized by air masses travelling mainly over sea ice (95% of the time) located in the North West side of the VRS station. By contrast, Fig. 3c–d shows that the NPF event detected in April are associated with air masses travelling almost exclusively over snow on Greenland land (86% of the time). The rest is associated to sea ice, and none to land without snow (0%) neither open ocean (0%). Finally, the NPF event detected in May had the majority of air masses travelling over sea ice regions (79%) with only a left minority over snow on land (21%), none over land or open ocean (0%). Arctic sea ice is a spatially complex physical environment - a vast biome composed of multiple habitats such as the upper and lower ice surfaces, snow cover, brine channels, melt ponds, ice openings and ice floes of all sizes, and the surrounding sea water. Sea ice satellite maps were investigated (Fig. 2 b, d, f) and it was found that for the air masses associated with May NPF events, they were travelling 65% of the time over consolidated full pack ice (100% cover) whereas they spent only 35% of the time over pack ice at 75–95% area cover.

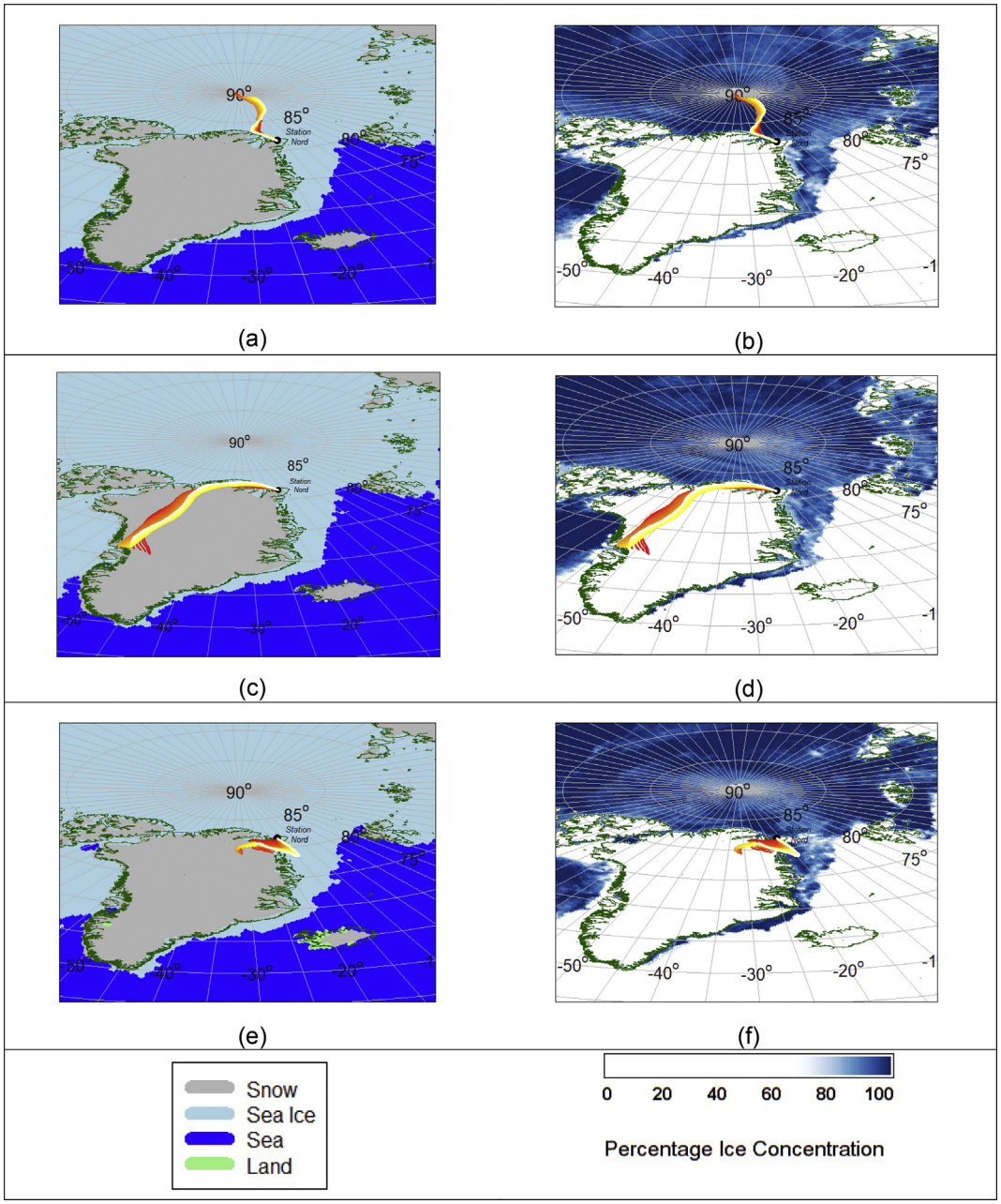

Fig. 2. Air mass back trajectories analysis for three selected events: (a, b) event of the 31 March 2015, (c, d) event of the 9–10 April 2015, and (e, f) event of the 22–23 May 2015). Maps show air mass travelling over two different satellite maps: (left maps) snow on land, land only, open ocean and sea ice and (right maps) sea ice regions (0–100% sea ice concentration). Average maps for the month of April–May 2015 are taken from the NOAA/NESDIS Interactive Multisensor Snow and Ice Mapping System (IMS).

3.3. Arctic NPF mechanisms

The current understanding of NPF mechanisms in the marine boundary layer over the Arctic Ocean is challenging due to the typically low concentration of nucleating agents. There is limited, but nonetheless useful information upon the chemistry of ultrafine particles during the growth phase of the frequently observed nucleation events through direct atmospheric ambient measurements. Recently developed research instruments have helped immensely in understanding the processes occurring in the 1–5 nm size range (Junninen et al., 2010; Sipilä et al., 2016). In this study, we only use the results obtained from the SP-AMS to report that accumulation mode chemical species detected in increased concentrations during the growth were also likely to be involved in the growth process of the nucleation mode.

The chemical composition of the nucleation stages herein detected is not known because the SP-AMS was not able to resolve masses in such small nanoparticle numbers. However, indirect evidence could be obtained from species detected in the concurrent larger submicron particles (Dall'Osto et al., 2012). Fig. 3 shows the temporal trends of SMPS and SP-AMS for three NPF events: (a) 31 March 2015, (b) 9–10 April 2015 and (c) 22–23 May 2015. For the considered periods, SP-AMS detected black carbon below detection limit, demonstrating clean Arctic conditions without any detectable anthropogenic influence. Additional information can be obtained by comparing average aerosol chemical measurements obtained by SP-AMS: nitrate, sulphate, organics and ammonium. The very low nitrate concentrations for early spring and late spring were below the limit of quantification. Sulphate was found to be the chemical species with highest aerosol loadings

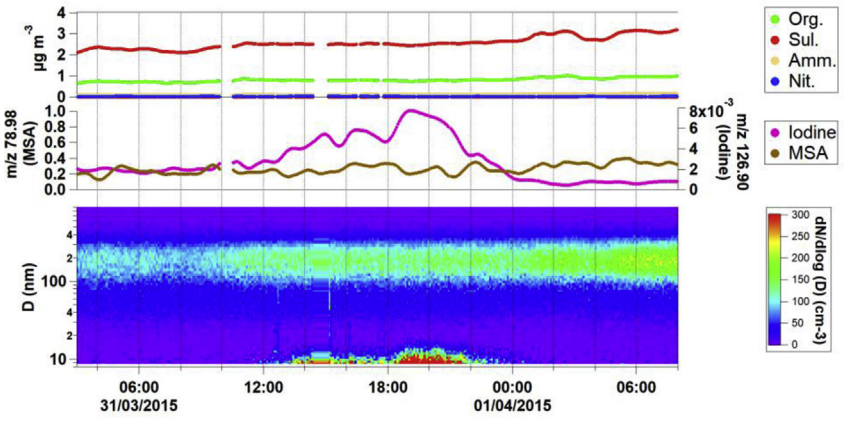

(a)

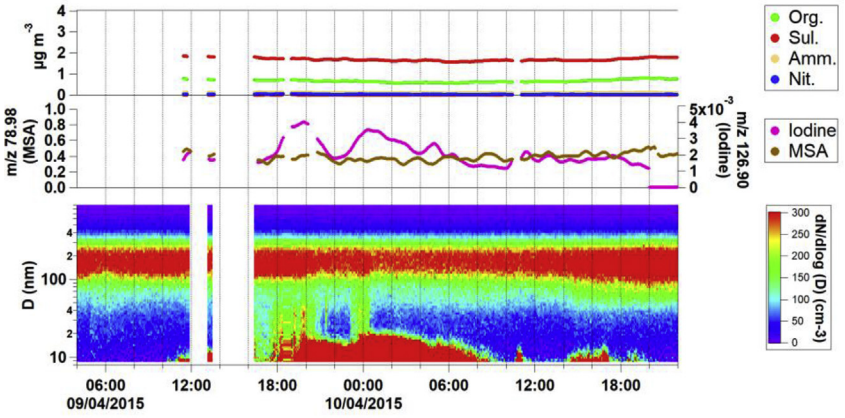

(b)

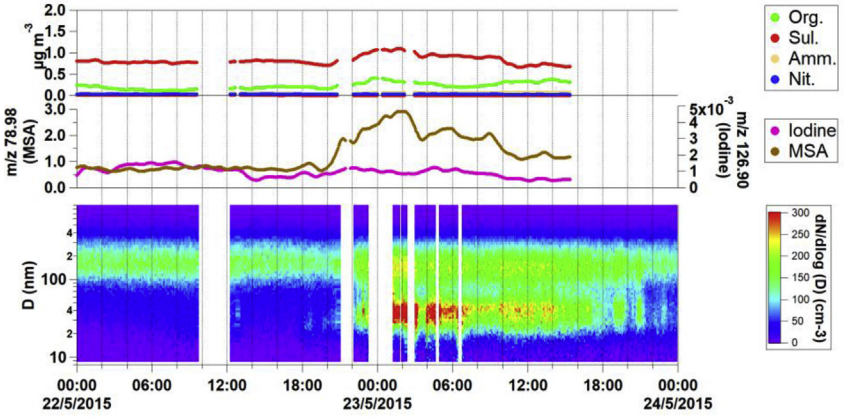

(c)

Fig. 3. Number-size distributions (bottom) and SP-AMS (top) temporal trends (local time) for three new particle formation events detected on (a) 31 March 2015 (as previously reported by Sippila et al., 2016 with API-TOF measurements), (b) 9–10 April 2015 and (c) 22–23 May 2015. Please note that the aerodynamic lens of the SP-AMS are capable of focussing. particles with 100% efficiency over a given range of aerodynamic diameters, in this case 30–700 nm, but smaller particles are not focussed correctly, hence the instrument is unable to directly measure these particles.

($1.1 \pm 0.44\,\mu g\,m^{-3}$), followed by organics ($0.46 \pm 0.21\,\mu g\,m^{-3}$) and ammonium ($0.01 \pm 0.03\,\mu g\,m^{-3}$). There was no statistical difference between the concentrations detected over the early spring events relative to the late spring ones.

In temperate marine and coastal environments, biogenic iodine, mostly in inorganic form, emitted from marine algae may control the formation of marine aerosols and cloud condensation nuclei (O'Dowd et al., 2002). Other marine biogenic components that have been shown to participate in aerosol nucleation are methyl-amines and methanesulfonic acid (MSA) (Dawson et al., 2012; Dall'Osto et al., 2012; Willis et al., 2016). We monitored MSA with the SP-AMS by quantifying the ion $CH_3SO_2^+$ (m/z 78.98) (Zorn et al., 2008; Ovadnevaite et al., 2014).

For iodine, the ion I^+ (m/z 126.90) has previously been reported as the largest peak in SP-AMS mass spectra of photochemically produced iodine oxide in the laboratory (Jimenez et al., 2003), and in ambient particles (Allan et al., 2015). Very good correlation (r = 0.92) between I^+ and IO^+ (m/z 143) in our study supports the validity of our iodine marker. Amines and organic nitrogen species (Dall'Osto et al., 2012; Willis et al., 2016) were found too close to detection limit and are not considered in this analysis. Iodine and MSA were found in very low concentrations during days characterized by Haze accumulation aerosol modes (Lange et al., 2018).

We assume the chemical composition changes observed in the growing accumulation mode particles results from condensation since all modes are growing simultaneously, and further, the condensing species is likely to be the same across all modes (Dall'Osto et al., 2012). However, different growth rates in different size particles have recently been reported in Arctic marine air (Burkart et al., 2017b). Looking at the constant background accumulation modes occurring during the three NPF events presented in Fig. 3a–c, it is reasonable to assume that some of the additional mass detected by the SP-AMS may be due to the aerosol mass of the NPF events. Fig. 3 shows increased signals of Iodine concomitant with NPF events detected on 31 March 2015 (Fig. 3a, same event reported in Sipilä et al., 2016 with a nitrate ion-based chemical ionization atmospheric pressure interface time-of flight - CI-APi-TOF - mass spectrometer measurements), and on 9–10 April (Fig. 3b), whereas an increase of MSA can be seen with grown particles detected on 22–23 May 2015 (Fig. 3c). Further information on possible NPF mechanisms and MSA-I sources can be found in the next two subsections.

3.3.1. Arctic iodine driven biotic and abiotic NPF

The association of iodine with Arctic NPF events is not new. Sipilä et al., 2016 reported direct molecular-level observations of nucleation in atmospheric field conditions monitored at our sampling location. Elevated concentrations of HIO_3 were observed after sunrise in late February, often associated with new particle formation events. During such events, the HIO_3 concentrations tended to be much higher than that of sulphuric acid, and it seems that the cluster formation could be explained almost entirely by the HIO_3 clustering mechanism. It is worth to remember also that Allan et al. (2015) pioneered an analysis of ship board NPF events observed in the Greenland Sea during the summertime. Using an Aerosol Mass Spectrometer (AMS), iodine was detected in the growing particles in one of the seven NPF events captured over coastal sea-ice. The NPF observations were putatively related to a potentially significant source of particles during periods of ice loss. It was stressed that if this phenomenon is limited to coastal areas, it would not explain NPF events above 80° N such as those reported by Karl et al. (2012).

Macroalgae have been identified as a source of molecular iodine in midlatitude coastal studies (Saiz-Lopez and Plane, 2004; Küpper et al., 2008), including in the northeast coast of Greenland (Borum et al., 2002). However, Northeast Greenland kelp beds are limited, especially in our winter-spring sampling period. Inorganic iodine from the marginal sea-ice zone has been previously reported (Atkinson et al., 2012), in particular ice diatoms have previously been shown to be a potential direct source of HOI and I_2 to the Arctic atmosphere (Hill and Manley, 2009). Microalgal aggregates released from melting sea-ice have also been proposed as an iodide source (Asmi et al., 2016; Boetius et al., 2013). Additional I_2 and HOI sources may also come by the abiotic oxidation of iodide, either by gaseous ozone on the sea surface (Carpenter et al., 2013; MacDonald et al., 2014), or within sea-ice brine channels followed by emissions from the quasi-liquid layer on the surface of the sea-ice (Saiz-Lopez and von Glasow, 2012). New ice formation leads to enrichment of halogens at the sea ice surface that readily can be oxidized to the highly volatile halogens (Cl_2, Br_2 and I_2 or a combination of them e.g. BrCl) (Saiz-Lopez et al., 2015; Simpson et al., 2015).

Despite these potential marine sources, the April NPF events were mainly associated with air masses travelling inland over snow. Very recently, Raso et al. (2017) reported the first measurements of molecular iodine (I_2) in the Arctic atmosphere and iodide (I^-) in the Arctic snowpack, and suggested that the coastal Arctic snowpack is capable of photochemical production and release of I_2 to the boundary layer. This was supported by enrichment of the snowpack in I^- compared to that expected from sea spray influence alone. Laboratory studies have previously shown that two mechanisms can produce and release inorganic iodine from snowpack to the atmosphere: i) production of I_2 and triiodide (I_3^-) through the photooxidation of iodide in ice (Kim et al., 2016), and ii) the heterogenous photoreduction of iodate in ice which leads to atmospheric emission of an iodine-containing photofragment (Gálvez et al., 2016). Combined, these experimental and field studies, along with the air mass origin, suggest that abiotic iodine production in snow/ice and subsequent release to the atmosphere is possibly related to the observed NPF events in April. It is also important to stress that previous particle growth observed in Greenland could not be explained by H_2SO_4 condensation, and were likely due to condensation of organic material. The source of condensing organic compounds was suggested to be snowpack emission following long-range transport and surface deposition (Ziemba et al., 2010). Significant concentrations of organic compounds have been measured in the snowpack in Greenland. For example, Anderson et al. (2008) reported gas-phase water soluble organic carbon (WSOC) concentrations in the firn that were more than a factor of ten larger than concentrations above the snowpack, suggesting that the snow surface was a source of gas-phase WSOC to the atmosphere. Further studies are needed in order to apportion the role or iodine and organic compounds.

3.3.2. Arctic MSA driven biotic and abiotic NPF

The NPF events detected in May, which were associated with air masses travelling over sea ice regions, concurred with higher concentrations of MSA. This compound arises from the atmospheric oxidation of the biogenic volatile DMS (Cox, 1997). DMS produced by marine phytoplankton is the most abundant form of sulphur released from the ocean (Simo, 2001). Associations between DMS flux, changes in sea ice extent and phytoplankton productivity are not fully understood. Sea ice is an organic sulphur-rich environment because ice algae generally contain high intracellular levels of dimethylsulfoniopropionate (DMSP) for osmoregulation and cryoprotection, and so do ice edge-associated phytoplankton (Levasseur, 2013). Therefore, the ice edge, particularly in the melting season (Leck and Persson, 1996) and open leads within the pack ice (Levasseur, 2013) can be strong sources of DMS. Previous studies (e.g., Becagli et al., 2016) have showed an increase in aerosol MSA in Arctic spring and summer, which results from the DMS source (Lana et al., 2011) as well as its photochemical oxidation and gas to particle conversion during transport.

Diagnostic and prognostic models fed with observations have estimated that DMS oxidation products (sulphate and MSA) make up roughly 10% of the accumulation mode aerosols (those in the size range and abundance with the highest potential to contribute to CCN numbers) annually in the Arctic (Vallina et al., 2007), a proportion that increases to one third in summer (Leaitch et al., 2013). Our results suggest that MSA may be involved either in the nucleation process itself, which is feasible if combined with alkaline biogenic compounds (Dawson et al., 2012), or in the first growth stages of the tiny newly born particles (Heintzenberg and Leck, 1994). In either case MSA may have a key role in regulating CCN numbers (Leaitch et al., 2013).

4. Conclusions

Fig. 4 summarise the NPF events selected, with air mass back trajectories analysis reported in Fig. 2 (Fig. 4a) and absolute SP-AMS signal for MSA and I_2 (Fig. 4b). Both species were found at higher concentrations (two fold) relative to Arctic "pristine" average

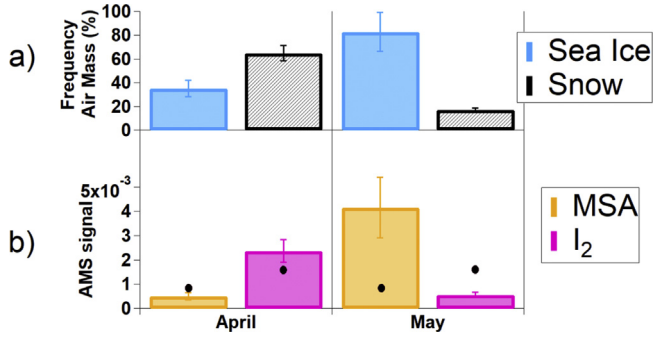

Fig. 4. (A) Summary of air mass back trajectories analysis reported in Fig. 2 and (b) absolute average daily signals SP-AMS signal for MSA and I_2 ($CH_3SO_2^+$, *m/z* 78.98 and I^+, *m/z* 126.90). Black dots represent average concentrations of relative chemical compounds for non NPF event days.

concentrations (black dots, Fig. 4), suggesting involvement in the NPF events detected. It is evident that whilst the April events presented higher signal for iodine than the May events, the latter presented higher signal for MSA. In summary, using an array of real time measurements taken at Station Nord over 88 days in 2015, we have demonstrated the occurrence of a number of NPF events occurring during spring for 7% of the time. The NPF events were associated with distinct air masses and surface characteristics: April events occurred in air masses that had travelled mostly over snow-covered land and sea ice regions, while May events were related mainly to sea ice regions. Measurements of aerosol chemical composition identified iodine and MSA as abundant species during NPF events, suggesting their role in either nucleation or early growth. While MSA has a well known biological origin in the ocean and sea ice (Lana et al., 2011; Levasseur, 2013; Becagli et al., 2016), iodine may originate in photochemical inorganic reactions in the snowpack, even on land (Raso et al., 2017). In a nutshell, our study supports the long described role of biogenic sulphur emissions on NPF as well as the recent findings pointing to abiotic release of iodine from snow. Additional sources from snow may come from snowpack emissions following long-range transport and surface deposition (Ziemba et al., 2010).

Given the dramatic impact of NPF events on the total particle number concentration in the Arctic environment, future work should aim to evaluate more carefully the molecular-level composition of candidate chemical compounds involved in aerosol nucleation and growth. It is very likely that a complex cocktail of chemical vapours originating from both biotic and abiotic processes is responsible for NPF events, depending on seasons and regions. These results once again call for a better representation of the exchanges between sea ice/ocean/snowpack and the atmosphere in Earth system models.

Acknowledgements

The study was supported by the Spanish Ministry of Economy through project BIO−NUC (CGL 2013–49020-R), PI−ICE (CTM 2017–89117-R) and the Ramon y Cajal fellowship (RYC-2012-11922). The National Centre for Atmospheric Science NCAS Birmingham group is funded by the UK Natural Environment Research Council. Thanks to the British Atmospheric Data Centre, which is part of the NERC National Centre for Atmospheric Science (NCAS), for the calculation of trajectories and access to ECMWF data. This work was financially supported by the Danish Environmental Protection Agency with means from the MIKA/DANCEA funds for Environmental Support to the Arctic Region, which is part of the Danish contribution to “Arctic Monitoring and Assessment Program” (AMAP) and to the Danish research project “Short lived Climate Forcers” (SLCF), and the Danish Council for Independent Research (project NUMEN, DFF-FTP-4005-00485B). The findings and conclusions presented here do not necessarily reflect the views of the Agency. This work was also supported by the Nordic Centre of Excellence (NCoE) Cryosphere-Atmosphere Interactions in a Changing Arctic Climate (CRAICC). The Villum Foundation is acknowledged for funding the construction of Villum Research Station, Station Nord. The authors are also grateful to the staff at Station Nord for their excellent and unwavering support.

References

Allan, J.D., Williams, P.I., Najera, J., Whitehead, J.D., Flynn, M.J., Taylor, J.W., Liu, D., Darbyshire, E., Carpenter, L.J., Chance, R., Andrews, S.J., Hackenberg, S.C., McFiggans, G., 2015. Iodine observed in new particle formation events in the Arctic atmosphere during ACCACIA. Atmos. Chem. Phys. 15, 5599–5609. https://doi.org/10.5194/acp-15-5599-2015.

Anderson, C.H., Dibb, J.E., Griffin, R.J., Hagler, G.S.W., Bergin, M.H., 2008. Atmospheric water-soluble organic carbon measurements at Summit, Greenland. Atmos. Environ. 42, 5612e5621.

Asmi, E., Kondratyev, V., Brus, D., Laurila, T., Lihavainen, H., Backman, J., Vakkari, V., Aurela, M., Hatakka, J., Viisanen, Y., Uttal, T., Ivakhov, V., Makshtas, A., 2016. Aerosol size distribution seasonal characteristics measured in Tiksi. Russian Arctic, Atmos. Chem. Phys 16, 1271–1287. https://doi.org/10.5194/acp-16-1271-2016.

Atkinson, H.M., Huang, R.-J., Chance, R., Roscoe, H.K., Hughes, C., Davison, B., Schönhardt, A., Mahajan, A.S., Saiz-Lopez, A., Hoffmann, T., Liss, P.S., 2012. Iodine emissions from the sea ice of the Weddell Sea. Atmos. Chem. Phys. 12, 11229–11244. https://doi.org/10.5194/acp-12-11229-2012.

Becagli, S., Lazzara, L., Marchese, C., Dayan, U., Ascanius, S.E., Cacciani, M., Caiazzo, L., Di Biagio, C., Di Iorio, T., di Sarra, A., Eriksen, P., Fani, F., Giardi, F., Meloni, D., Muscari, G., Pace, G., Severi, M., Traversi, R., Udisti, R., 2016. Relationshipslinking prymary production, sea ice melting, and biogenic aerosol inthe Arctic. Atmos. Environ. 136, 1e15. https://doi.org/10.1016/j.atmosenv.2016.04.002.

Beddows, D.C.S., Dall'Osto, M., Harrison, R.M., 2009. Cluster analysis of rural, urban and curbside atmospheric particle size data. Environ. Sci. Technol. 43, 4694–4700.

Boetius, A., Albrecht, S., Bakker, K., Bienhold, C., Felden, J., Fernandez-Mendez, M., Hendricks, S., Katlein, C., Lalande, C., Krumpen, T., Nicolaus, M., Peeken, I., Rabe, B., Rogacheva, A., Rybakova, E., Somavilla, R., Wenzhofer, F., Polarstern, R.V., 2013. ARK27-3-Shipboard Science party: Export of algal Biomass from the melting arctic sea ice. Science 339, 1430–1432. https://doi.org/10.1126/science.1231346.

Borum, J., Pedersen, M.F., Krause-Jensen, D., Christensen, P.B., Nielsen, K., 2002. Biomass, photosynthesis and growth of Laminaria saccharina in a high-arctic fjord, NE Greenland. Mar. Biol.,141 11–19. https://doi.org/10.1007/s00227-002-0806-9.

Burkart, J., Willis, M.D., Bozem, H., Thomas, J.L., Law, K., Hoor, P., Aliabadi, A.A., Köllner, F., Schneider, J., Herber, A., Abbatt, J.P.D., Leaitch, W.R., 2017a. Summertime observationsof elevated levels of ultrafine particles in the high Arctic marine boundary layer. Atmos. Chem. Phys. 17, 5515–5535. https://doi.org/10.5194/acp-17-5515-2017.

Burkart, J., Hodshire, A.L., Mungall, E.L., Pierce, J.R., Collins, D.B., Ladino, L.A., Lee, A.K.Y., Irish, V., Wentzell, J.J.B., Liggio, J., Papakyriakou, T., Murphy, J., Abbatt, J., 2017b. Organic condensation and particle growth to CCN sizes in the summertime marine Arctic is driven by materials more semivolatile than at continental sites. Geophys. Res. Lett. 44, 10725–10734. https://doi.org/10.1002/2017GL075671.

Carpenter, L.J., MacDonald, S.M., Shaw, M.D., Kumar, R., Saunders, R.W., Parthipan, R., Wilson, J., Plane, J.M.C., 2013. Atmospheric iodine levels influenced by sea surface emissions of inorganic iodine. Nat. Geosci. 6, 108–111. https://doi.org/10.1038/Ngeo1687.

Carslaw, K.S., Lee, L.A., Reddington, C.L., Pringle, K.J., Rap, A., Forster, P.M., Mann, G.W., Spracklen, D.V., Woodhouse, M.T., Regayre, L.A., Pierce, J.R., 2013. Large contribution ofnatural aerosols to uncertainty in indirect forcing. Nature 503, 67–71. https://doi.org/10.1038/nature12674.

Charlson, R.J., Lovelock, J.E., Andreae, M.O., Warren, S.G., 1987. Oceanic phyto-plankton, atmospheric sulfur, cloud albedo and climate. Nature 326, 655–661. https://doi.org/10.1038/326655a0.

Collins, D.B., Burkart, J., Chang, R.Y.-W., Lizotte, M., Boivin-Rioux, A., Blais, M., Mungall, E.L., Boyer, M., Irish, V.E., Massé, G., Kunkel, D., Tremblay, J.-É., Papakyriakou, T., Bertram, A.K., Bozem, H., Gosselin, M., Levasseur, M., Abbatt, J.P.D., 2017. Frequent ultrafine particle formation and growth in Canadian Arctic marine and coastal environments. Atmos. Chem. Phys. 17, 13119–13138. https://doi.org/10.5194/acp-17-13119-2017.

Cox, R.A., 1997. Atmospheric sulphur and climate: what have we learned? Philos. Trans. R. Soc., Ser. B 352, 251–254.

Croft, B., Wentworth, G.R., Martin, R.V., Leaitch, W.R., Murphy, J.G., Murphy, B.N., Kodros, J.K., Abbatt, J.P.D., Pierce, J.R., 2016. Contribution of Arctic seabird-colony ammonia to atmospheric particles and cloud-albedo radiative effect. Nat. Commun. 7, 13444. https://doi.org/10.1038/ncomms13444.

Dall'Osto, M., Querol, X., Alastuey, A., O'Dowd, C., Harrison, R.M., Wenger, J., Gómez-Moreno, F.J., 2013. On the spatial distribution and evolution of ultrafine particles in Barcelona. Atmos. Chem. Phys. 13, 741–759. https://doi.org/10.5194/acp-13-741-2013.

Dall'Osto, M., Beddows, D.C.S., Asmi, A., Poulain, L., Hao, L., Freney, E., Allan, J.D., Canagaratna, M., Crippa, M., Bianchi, F., de Leeuw, G., Eriksson, A., Swietlicki, E., Hansson, H.C., Henzing, J.S., Granier, C., Zemankova, K., Laj, P., Onasch, T., Prevot, A., Putaud, J.P., Sellegri, K., Vidal, M., Virtanen, A., Simo, R., Worsnop, D., O'Dowd, C., Kulmala, M., Harrison, R.M., 2018. Novel insights on new particle formation derived from a pan-european observing system. Sci. Rep. 8 (1), 1482. https://doi.org/10.1038/s41598-017-17343-9. 2018a Jan 24.

Dall'Osto, M., Geels, C., Beddows, D.C.S., Boertmann, D., Lange, R., Nøjgaard, J.K., Harrison Roy, M., Simo, R., Skov, H., Massling, A., 2018b. Regions of open water and melting sea ice drive new particle formation in North East Greenland. Sci. Rep. 8, 6109.

Dall'Osto, M., Beddows, D.C.S., Tunved, P., Krejci, R., Ström, J., Hansson, H.-C., Yoon, Y.J., Park, Ki-Tae, Becagli, S., Udisti, R., Onasch, T., O'Dowd, C.D., Simó, R., Harrison, Roy M., 2017a. Arctic sea ice melt leads to atmospheric new particle formation. 2017a. Scientific Reports 7, Article number 3318. https://doi.org/10.1038/s41598-017-03328-1.

Dall'Osto, M., Monahan, C., Greaney, R., Beddows, D.C.S., Harrison, R.M., Ceburnis, D., O'Dowd, C.D., 2011. A statisticalanalysis of North East Atlantic (submicron) aerosol size distributions. Atmos. Chem. Phys. 11, 12567–12578. https://doi.org/10.5194/acp-11-12567-2011.

Dall'Osto, M., Ceburnis, D., Monahan, C., Worsnop, D.R., Bialek, J., Kulmala, M., Kurtén, T., Ehn, M., Wenger, J., Sodeau, J., Healy, R., O'Dowd, C., 2012. Nitrogenated andaliphatic organic vapors as possible drivers for marine secondaryorganic aerosol growth. J. Geophys. Res. Atmos. 117, D12311. https://doi.org/10.1029/2012JD017522.

Dall'Osto, M., Ovadnevaite, J., Paglione, M., Beddows, D.C.S., Ceburnis, D., Cree, C., Cortés, P., Zamanillo, M., Nunes, S.O., Pérez, G.L., Ortega-Retuerta, E., Emelianov, M., Vaqué, D., Marrasé, C., Estrada, M., Montserrat Sala, M., Vidal, M., Fitzsimons, M.F., Beale, R., Airs, R., Rinaldi, M., Decesari, S., Facchini, M.C., Harrison, R.M., O'Dowd, C., Simó, R., 2017b. Antarctic sea ice region as a source of biogenic organic nitrogen in aerosols. Sci. Rep. 7 6047. https://doi.org/10.1038/s41598-017-06188-x.

Dawson, M.L., Varner, M.E., Perraud, V., Ezell, M.J., Gerber, R.B., Finlayson-Pitts, B.J., 2012. Simplified mechanism for new particle formation from methanesulfonic acid, amines, and water via experiments and ab initio calculations. P. Natl. Acad. Sci. USA 109, 18719–18724.

DeCarlo, P.F., Kimmel, J.R., Trimborn, A., Northway, M.J., Jayne, J.T., Aiken, A.C., Gonin, M., Fuhrer, K., Horvath, T., Docherty, K.S., Worsnop, D.R., Jimenez, J.L., 2006. Field-deployable, high-resolution, time-of-flight aerosol mass spectrometer. Anal. Chem. 78, 8281–8289.

Freud, E., Krejci, R., Tunved, P., Leaitch, R., Nguyen, Q.T., Massling, A., Skov, H., Barrie, L., 2017. Pan-Arctic aerosol number size distributions: seasonality and transport patterns. Atmos. Chem. Phys. 17, 8101–8128. https://doi.org/10.5194/acp-17-8101-2017.

Gálvez, Ó., Baeza-Romero, M.T., Sanz, M., Saiz-Lopez, A., 2016. Photolysis of frozen iodate salts as a source of active iodine in the polar environment. Atmos. Chem. Phys. 16, 12703–12713.

Heintzenberg, J., Leck, C., 1994. Seasonal variations of the atmospheric aerosol near the top of the marine boundary layer over Spitsbergen related to the Arctic sulfur cycle. Tellus 46B, 52–67.

Heintzenberg, J., Leck, C., 2012. The summer aerosol in the central Arctic 1991–2008: did it change or not? Atmos. Chem. Phys. 12 (9), 3969–3983. https://doi.org/10.5194/acp-12-3969-2012.

Heintzenberg, J., Leck, C., Tunved, P., 2015. Potential source regions and processes of aerosol in the summer Arctic. Atmos. Chem. Phys. 15 (11), 6487–6502. https://doi.org/10.5194/acp-15-6487-2015.

Hill, V.L., Manley, S.L., 2009. Release of reactive bromine and iodine from diatoms and its possible role in halogen transfer in polar and tropical oceans. Limnol. Oceanogr. 54, 812–822. https://doi.org/10.4319/lo.2009.54.3.0812.

Intrieri, J.M., Fairall, C.W., Shupe, M.D., Persson, P.O.G., Andreas, E.L., Guest, P.S., Moritz, R.E., 2002. Annual cycle of Arctic surface cloud forcing at SHEBA. J. Geophys. Res. 107https://doi.org/10.1029/2000JC000439. C10.

Jimenez, J.L., Bahreini, R., Cocker, D.R., Zhuang, H., Varutbangkul, V., Flagan, R.C., Seinfeld, J.H., O'Dowd, C.D., Hoffmann, T., 2003. New particle formation fromphotooxidation of diiodomethane (CH2I2). Journal of GeophysicalResearch -Atmospheres 108 (D10) art. no.-4318.

Junninen, H., Ehn, M., Petäjä, T., Luosujärvi, L., Kotiaho, T., Kostiainen, R., Rohner, U., Gonin, M., Fuhrer, K., Kulmala, M., Worsnop, D.R., 2010. A high-resolution mass spectrometer to measure atmospheric ion composition. Atmos. Meas. Tech. 3, 1039–1053. https://doi.org/10.5194/amt-3-1039-2010.

Karl, M., Leck, C., Gross, A., Pirjola, L., 2012. A study of new particle formation in the marine boundary layer over the central Arctic Ocean using a flexible multicomponent aerosol dynamic model. Tellus B 64, 17158,. https://doi.org/10.3402/Tellusb.V64i0.17158.

Kim, K., Yabushita, A., Okumura, M., Saiz-Lopez, A., Cuevas, C.A., Blaszczak-Boxe, C.S., Min, D.W., Yoon, H.-I., Choi, W., 2016. Production of molecular iodine and triiodide in the frozen solutionof iodide: implication for polar atmosphere. Environ. Sci. Technol. 50, 1280–1287. https://doi.org/10.1021/acs.est.5b05148.

Köllner, F., Schneider, J., Willis, M.D., Klimach, T., Helleis, F., Bozem, H., Kunkel, D., Hoor, P., Burkart, J., Leaitch, W.R., Aliabadi, A.A., Abbatt, J.P.D., Herber, A.B., Borrmann, S., 2017. Particulate trimethylamine in the summertime Canadian high Arctic lower troposphere. Atmos. Chem. Phys. 17, 13747–13766. https://doi.org/10.5194/acp-17-13747-2017.

Kulmala, M., Vehkamaki, H., Petajda, T., Dal Maso, M., Lauri, A., Kerminen, V.M., Birmili, W., McMurry, P.H., 2004. Formationand growth rates of ultrafine atmospheric particles: a review of observations. J. Aerosol Sci. 35, 143–176.

Küpper, F.C., Carpenter, L.J., McFiggans, G.B., Palmer, C.J., Waite, T.J., Boneberg, E.-M., Woitsch, S., Weiller, M., Abela, R., Grolimund, D., Potin, P., Butler, A., Luther, G.W., Kroneck, P.M.H., Meyer-Klaucke, W., Feiters, M.C., 2008. Iodide accumulationprovides kelp with an inorganic antioxidant impactingatmospheric chemistry. Proc. Natl. Acad. Sci. Unit. States Am. 105, 6954–6958. https://doi.org/10.1073/pnas.0709959105.

Lana, A., Bell, T.G., Simó, R., Vallina, S.M., Ballabrera-Poy, J., Kettle, A.J., Dachs, J., Bopp, L., Saltzman, E.S., Stefels, J., Johnson, J.E., Liss, P.S., 2011. An updated climatology of surface dimethlysulfide concentrations and emission fluxes in the global ocean. Glob. Biogeochem. Cycles 25, GB1004. https://doi.org/10.1029/2010GB003850.

Lange, R., Dall'Osto, M., Skov, H., Nøjgaard, J.K., Nielsen, I.E., Beddows, D.C.S., Simo, R., Harrison, R.M., Massling, A., 2018. Characterization of distinct Arctic aerosol accumulation modes and their sources. Atmos. Environ. 183 (2018), 1–10.

Leaitch, W.R., Sharma, S., Huang, L., Toom-Sauntry, D., Chivulescu, A., Macdonald, A.M., von Salzen, K., Pierce, J.R., Bertram, A.K., Schroder, J.C., Shantz, N.C., Chang, R.Y.-W., Norman, A.-L., 2013. Dimethyl sulfide control of the clean summertime Arctic aerosol and cloud. Elementa: Science of the Anthropocene 1https://doi.org/10.12952/journal.elementa.000017. 000017.

Leaitch, W.R., Russell, L.M., Liu, J., Kolonjari, F., Toom, D., Huang, L., Sharma, S., Chivulescu, A., Veber, D., Zhang, W., 2018. Organic functional groups in the submicron aerosol at 82.5° N, 62.5° W from 2012 to 2014. Atmos. Chem. Phys. 18, 3269–3287. https://doi.org/10.5194/acp-18-3269-2018.

Leck, C., Bigg, E.K., 1999. Aerosol production over remote marine areas—a new route. Geophys. Res. Lett. 26 (23), 3577–3580. https://doi.org/10.1029/1999GL010807.

Leck, C., Persson, C., 1996. The central Arctic Ocean as a source of dimethyl sulfide: seasonal variability in relation to biological activity. Tellus B 48, 156–177.

Levasseur, M., 2013. Impact of Arctic meltdown on the microbial cycling of sulphur. Nat. Geosci. 6, 691–700.

MacDonald, S.M., Gómez Martín, J.C., Chance, R., Warriner, S., Saiz-Lopez, A., Carpenter, L.J., Plane, J.M.C., 2014. A laboratory characterisation of inorganic iodine emissions from the sea surface: dependence on oceanic variables and parameterisation for global modelling. Atmos. Chem. Phys. 14, 5841–5852. https://doi.org/10.5194/acp-14-5841-2014.

Merikanto, J., Spracklen, D.V., Mann, G.W., Pickering, S.J., Carslaw, K.S., 2009. Impact of nucleation on global CCN. Atmos. Chem. Phys. 9, 8601–8616. https://doi.org/10.5194/acp-9-8601-2009.

Mungall, E.L., Abbatt, J.P.D., Wentzell, J.J.B., Lee, A.K.Y., Thomas, J.L., Blaise, M., Gosselin, M., Miller, L.M., Papakyriakou, T., Willis, M.D., Liggio, J., 2017. Source of oxygenated volatile organic compounds in the summertime marine Arctic boundary layer. P. Natl. Acad. Sci. USA 24, 6203–6208. https://doi.org/10.1073/pnas.1620571114.

Nguyen, Q.T., et al., 2013. Source apportionment of particles at station Nord, north East Greenland during 2008-2010 using COPREM and PMF analysis. Atmos. Chem. Phys. 13, 35–49. https://doi.org/10.5194/acp-13-35-2013.

Nguyen, Q.T., et al., 2016. Seasonal variation of atmospheric particle number concentrations, new particle formation and atmospheric oxidation capacity at the high Arctic site Villum Research Station, Station Nord. Atmos. Chem. Phys. 16, 11319–11336. https://doi.org/10.5194/acp-16-11319-2016.

Onasch, T.B., Trimborn, A., Fortner, E.C., Jayne, J.T., Kok, G.L., Williams, L.R., Davidovits, P., Worsnop, D.R., 2012. Soot particle aerosol mass spectrometer: Development, Validation, and initial Application. Aerosol Sci. Technol. 46, 804–817.

Ovadnevaite, J., Ceburnis, D., Leinert, S., Dall'Osto, M., Canagaratna, M., O'Doherty, S., Berresheim, H., O'Dowd, C., Submicron, N.E., 2014. Atlantic marine aerosol chemical composition and abundance:Seasonal trends and air mass categorization. J. Geophys. Res. Atmos. 119, 11,850–11,863. https://doi.org/10.1002/2013JD021330.

O'Dowd, C.D., Jimenez, J.L., Bahreini, R., Flagan, R.C., Seinfeld, J.H., Pirjola, L., Kulmala, M., Jennings, S.F.G., Hoffmann, T., 2002. Marine particle formation from biogenic iodine emissions. Nature 417, 632–636.

Ramanathan, V., Crutzen, P.J., Kiehl, J.T., Rosenfeld, D., 2001. Aerosols, climate, and the Hydrological cycle. Science 294 (5549).

Raso, A.K., Custard, D., May, N.W., Tanner, D., Newburn, M.K., Walker, L., Moore, R.J., Huey, L.G., Alexander, L., Shepson, P.B., Pratt, K.A., 2017. Active molecular iodine photochemistry in the Arctic. www.pnas.org/cgi/doi/10.1073/pnas.1702803114.

Saiz-Lopez, A., von Glasow, R., 2012. Reactive halogen chemistry in the troposphere. Chem. Soc. Rev. 41, 6448–6472. https://doi.org/10.1039/c2cs35208g.

Saiz-Lopez, A., Plane, J.M.C., 2004. Novel iodine chemistry in the marine boundary layer. Geophys. Res. Lett. 31 04110.01029/02003GL019215, L04112.

Saiz-Lopez, A., Blaszczak-Boxe, C.S., Carpenter, L.J., 2015. A mechanism for biologically-induced iodine emissions fromsea-ice. Atmos. Chem. Phys. Discuss. 15, 10257–10297. https://doi.org/10.5194/acpd-15-10257-2015.

Schwarz, J.P., Spackman, J.R., Gao, R.S., Perring, A.E., Cross, E., Onasch, T.B., et al., 2010. The detection efficiency of the single particle Soot Photometer. Aerosol Sci. Technol. 44, 612–628.

Serreze, M.C., Stroeve, J., 2015. Arctic sea ice trends, variability and implications for seasonal ice forecasting. Philos. Transact. A Math. Phys. Eng. Sci. 373 (2045). https://doi.org/10.1098/rsta.2014.0159.

Simo, R., 2001. Production of atmospheric sulfur by oceanic plankton: biogeochemical, ecological and evolutionary links. Trends Ecol. Evol. 16 (6) 287e294. https://doi.org/10.1016/S0169-5347(01)02152-8.

Simpson, W.R., Brown, S.S., Saiz-Lopez, A., Thornton, J.A., von Glasow, R., 2015. Tropospheric halogen chemistry:sources, cycling, and impacts. Chem. Rev. 115, 4035–4062. https://doi.org/10.1021/cr5006638.

Sipilä, M., Sarnela, N., Jokinen, T., Henschel, H., Junninen, H., Kontkanen, J., Richters, S., Kangasluoma, J., Franchin, A., 5 Peräkylä, O., Rissanen, M.P., Ehn, M., Vehkamäki, H., Kurten, T., Berndt, T., Petäjä, T., Worsnop, D., Ceburnis, D., Kerminen, V.-M., Kulmala, M., O'Dowd, C., 2016. Molecular-scale evidence of aerosol particle formation via sequential addition of HIO3. Nature 537, 532–534. https://doi.org/10.1038/nature19314.

Spracklen, D.V., Carslaw, K.S., Kulmala, M., Kerminen, V.-M., Mann, G.W., Sihto, S.-L., 2006. The contribution of boundarylayer nucleation events to total particle concentrations on regional and global scales. Atmos. Chem. Phys. 6, 5631–5648. https://doi.org/10.5194/acp-6-5631-2006.

Ström, J., Engvall, A.-C., Delbart, F., Krejci, R., Treffeisen, R., 2011. On small particles in the Arctic summer boundary layer: observations at two different heights near Ny-Alesund, Svalbard. Tellus B 61 (2), 473–482.

Tunved, P., Ström, J., Krejci, R., 2013. Arctic aerosol life cycle: linking aerosol size distributions observed between 2000 and 2010 with air mass transport and precipitation at Zeppelin station, Ny-Ålesund, Svalbard. Atmos. Chem. Phys. 13, 3643–3660.

Vallina, S.M., Simó, R., Gassó, S., de Boyer-Montégut, C., del Río, E., Jurado, E., Dachs, J., 2007. Analysis of a potential "solar radiation dose–dimethylsulfide–cloud condensation nuclei" link from globally mapped seasonal correlations. Global Biogeochem. Cycles 2d1https://doi.org/10.1029/2006GB002787. GB2004.

Weber, R.J., McMurry, P.H., Mauldin, L., Tanner, D.J., Eisele, F.L., Brechtel, F.J., Kreidenweis, S.M., Kok, G.L., Schillawski, R.D., Baumgardner, D., 1998. A study of new particle formation and growth involving biogenic and trace gas species measured during ACE 1. J. Geophys. Res. Atmos. 103, 16385–16396. https://doi.org/10.1029/97JD02465.

Wiedensohler, A., Covert, D.S., Swietlicki, E., Aalto, P., Heintzenberg, J., Leck, C., 1996. Occurrence of an ultrafine particle mode less than 20 nm in diameter in the marine boundary layer during Arctic summer and autumn. Tellus Ser. B Chem. Phys. Meteorol. 48 (2), 213–222. https://doi.org/10.1034/j.1600-0889.1996.t01-1-00006.x.

Willis, M.D., Burkart, J., Thomas, J.L., Köllner, F., Schneider, J., Bozem, H., Hoor, P.M., Aliabadi, A.A., Schulz, H., Herber, A.B., Leaitch, W.R., Abbatt, J.P.D., 2016. Growth of nucleationmode particles in the summertime Arctic: a case study. Atmos. Chem. Phys. 16, 7663–7679. https://doi.org/10.5194/acp-16-7663-2016.

Willis, M.D., Burkart, J., Bozem, H., Thomas, J.L., Aliabadi, A.A., Hoor, P.M., Schulz, H., Herber, A.B., Leaitch, W.R., Abbatt, J.P.D., 2017. Evidence for marine-biogenic influence on summertime Arctic aerosol. Geophys. Res. Lett. 44, 6460–6470. https://doi.org/10.1002/2017GL073359.

Ziemba, L.D., Dibb, J.E., Griffin, R.J., Huey, L.G., Beckman, P., 2010. Observations of particle growth at a remote, Arctic site. Atmos. Environ. 44 (13), 1649–1657. https://doi.org/10.1016/j.atmosenv.2010.01.032.

Zorn, S.R., Drewnick, F., Schott, M., Hoffmann, T., Borrmann, S., 2008. Characterization of the South Atlantic marine boundary layer aerosol using an aerodyne aerosol mass spectrometer. Atmos. Chem. Phys. 8 (16), 4711–4728.